

Self-learning active noise control

J. Yuan^{a)}

Department of Mechanical Engineering, The Hong Kong Polytechnic University, Hunghom, Kowloon, Hong Kong

(Received 12 September 2007; revised 8 May 2008; accepted 16 July 2008)

An important step for active noise control (ANC) systems to be practical is to develop model independent ANC (MIANC) systems that tolerate parameter variations in sound fields. Reliabilities and stabilities of many MIANC systems depend on results of online system identifications. Parameter errors due to system identifications may threaten closed-loop stabilities of MIANC systems. A self-learning active noise control (SLANC) system is proposed in this study to stabilize and optimize an ANC system in case identified parameters are unreliable. The proposed system uses an objective function to check closed-loop stability. If partial or full value of the objective function exceeds a conservatively preset threshold, a stability threat is detected and the SLANC system will stabilize and optimize the controller without using parameters of sound fields. If the reference signal is available, the SLANC system can be combined with a feedforward controller to generate both destructive interference and active damping in sound fields. The self-learning method is simple and stable for many feedback ANC systems to deal with a worst case discussed in this study.

© 2008 Acoustical Society of America. [DOI: 10.1121/1.2968700]

PACS number(s): 43.50.Ki [BSF]

Pages: 2078–2084

I. INTRODUCTION

It has been demonstrated by many researchers that active noise control (ANC) is an effective way of suppressing low-frequency noise. The principle of ANC is either destructive interference by feedforward control, or active damping by feedback control.^{1,2} It is possible to combine feedforward/feedback control to generate both destructive interference and active damping in sound fields. Feedforward control is applicable to a sound field if (a) the reference signal is available or recoverable, and (b) primary source and secondary actuator(s) are in upstream locations with respect to an intended quiet zone. In some applications, it is possible to separate reflected waves from incident waves. Feedforward control may be applied to cancel reflected waves for sound absorption. If the reference signal is not available, feedback control is preferred to generate active damping in sound fields. In three-dimensional sound fields or vibration systems, active damping may be more suitable since it does not require the reference signal and separation of incident/reflected waves.

Accurate models of sound fields are very important in generating destructive (instead of constructive) interference or positive (instead of negative) damping. Model independent ANC (MIANC) systems depend on results of online system identifications or invariant properties of sound fields to ensure stabilities. Examples of feedback MIANC systems are direct rate feedback controllers or active resonators, which are theoretically stable in sound fields if dynamics of electronic circuits are negligible.^{3–6} In reality, dynamics of electronic circuits are not necessarily negligible and may cause stability problems to direct rate feedback controllers or active resonators. Many direct rate feedback controllers and

active resonators require collocated feedback signals. Suppressing collocated feedback signals does not necessarily mean suppressing signals measured away from speakers.

In this study, a self-learning ANC (SLANC) system is proposed as an alternative way to deal with existing problems in feedback MIANC systems. The SLANC system does not require collocated feedback and tolerates dynamic uncertainties (including dynamics of electronic circuits) to ensure closed-loop stability. It is also able to minimize an objective function by tuning controller parameters without using parameters of sound fields. If the reference signal is available, the SLANC system may be integrated with a feedforward controller to generate both destructive interference and active damping in sound fields. Theoretical analysis and experimental results are presented to demonstrate stability and effectiveness of the SLANC system.

II. MODEL OF RESONANT SOUND FIELDS

Since active damping is most suitable for resonant sound fields, the modal theory is adopted to model resonant sound fields. One may consider an ANC system with a primary source at point x_p , a secondary actuator at point x_a , a feedback sensor at point x_f , and an error sensor at point x_e . Let $\phi_k(x)$ denote the k th eigenfunction of a sound field and $q_k(t)$ denote the corresponding temporal coordinate. The pressure signal, measured by the error sensor, may be expressed as^{1,2}

$$p(x_e, t) = \sum_{k=1}^m \phi_k(x_e) q_k(t). \quad (1)$$

Equation (1) is theoretically an infinite summation. Practically, it is truncated to the first m modes. The signal model is applicable to pressure signals measured at other points such as the feedback point x_f . The only modification is to replace x_e with spatial coordinate of the measurement point such as

^{a)}Electronic mail: mmjyuan@polyu.edu.hk

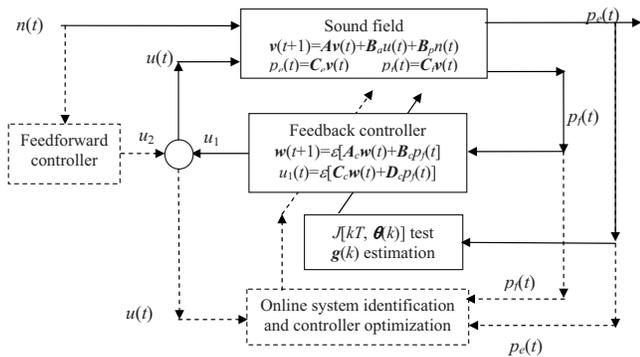


FIG. 1. Block diagram of the closed-loop SLANC system.

$$\mathbf{v}(t+1) = \mathbf{A}\mathbf{v}(t) + \mathbf{B}_a u(t) + \mathbf{B}_p n(t), \quad (10)$$

$$p_e(t) = \mathbf{C}_e \mathbf{v}(t), \quad p_f(t) = \mathbf{C}_f \mathbf{v}(t). \quad (11)$$

Equations (10) and (11) include dynamics of sensors, actuators, and electronic circuits. It is customary to assume $\delta t = 1$, without any negative effects to the general case of $\delta t \neq 1$.

Unlike \mathbf{A}_0 , \mathbf{B}_{0a} , \mathbf{B}_{0p} , \mathbf{C}_{0e} , and \mathbf{C}_{0f} in the continuous-time model, \mathbf{A} , \mathbf{B}_a , \mathbf{B}_p , \mathbf{C}_e , and \mathbf{C}_f contain complicated and unknown parameters, some of which may not have analytical expressions. Stability of a SLANC system only depends on eigenvalues of \mathbf{A} that are all inside the unit circle centered at the origin of a complex plane. This is an invariant property of discrete-time models of sound fields that are open-loop stable with bounded outputs when excited by bounded inputs. Mathematically, it implies the existence of positive definite matrices $\mathbf{P} = \mathbf{P}^T > 0$ and $\mathbf{Q} = \mathbf{Q}^T > 0$,^{7,10,11,13} such that

$$\mathbf{P} - \mathbf{A}^T \mathbf{P} \mathbf{A} = \mathbf{Q} > 0. \quad (12)$$

The closed-loop SLANC system is described by a block diagram in Fig. 1. The actuation signal consists of two parts $u(t) = u_1(t) + u_2(t)$, where $u_1(t)$ is the feedback part and $u_2(t)$ is an optional feedforward part. The signals are synthesized by two blocks in Fig. 1. The dashed block, labeled “feedforward controller,” generates the optional $u_2(t)$ only if $n(t)$ is available as the reference signal. The main focus of this study is $u_1(t)$, synthesized by the solid block of “feedback controller.” The corresponding control law is

$$\mathbf{w}(t+1) = \varepsilon [\mathbf{A}_c \mathbf{w}(t) + \mathbf{B}_c p_f(t)], \quad (13)$$

$$u_1(t) = \varepsilon [\mathbf{C}_c \mathbf{w}(t) + \mathbf{D}_c p_f(t)], \quad (14)$$

where $\varepsilon > 0$ is a tunable parameter; elements of \mathbf{A}_c , \mathbf{B}_c , \mathbf{C}_c , and \mathbf{D}_c may be initialized with random numbers and tuned by two possible algorithms. One is the combination of available online system identification and controller optimization algorithms, represented by the dashed tuning block in Fig. 1; the other is a self-learning algorithm, represented by the solid tuning block in Fig. 1. The self-learning objective is to minimize

$$J(kT, \boldsymbol{\theta}) = \frac{1}{T} \sum_{i=kT}^{(k+1)T} p_e^2(i), \quad (15)$$

where T is the number of signal samples in a sufficiently long averaging period; $\boldsymbol{\theta}$ is a vector with one-to-one mapping

to elements of \mathbf{A}_c , \mathbf{B}_c , \mathbf{C}_c , and \mathbf{D}_c . The proposed system is based on an assumption that

$$J(kT, \boldsymbol{\theta}) \approx J(T, \boldsymbol{\theta}) \approx J(\boldsymbol{\theta}) = E\{p_e^2 | \boldsymbol{\theta}\} \quad (16)$$

for all integer k if the averaging period T is sufficiently long. This is applicable to sound fields with stationary and ergodic noise sources.

One may derive the model of closed-loop system by combining models of the sound field, Eqs. (10) and (11), and the controller, Eqs. (13) and (14). The result is given by^{7,10,11,13}

$$\begin{bmatrix} \mathbf{v}(t+1) \\ \mathbf{w}(t+1) \end{bmatrix} = \begin{bmatrix} \mathbf{A} + \varepsilon \mathbf{B}_a \mathbf{D}_c \mathbf{C}_f & \varepsilon \mathbf{B}_a \mathbf{C}_c \\ \varepsilon \mathbf{B}_c \mathbf{C}_f & \varepsilon \mathbf{A}_c \end{bmatrix} \begin{bmatrix} \mathbf{v}(t) \\ \mathbf{w}(t) \end{bmatrix} + \begin{bmatrix} \mathbf{B}_p \\ \mathbf{B}_a \end{bmatrix} n(t) + \begin{bmatrix} \mathbf{B}_a \\ \mathbf{0} \end{bmatrix} u_2(t), \quad (17)$$

$$p_e(t) = [\mathbf{C}_e] \begin{bmatrix} \mathbf{v}(t) \\ \mathbf{w}(t) \end{bmatrix}. \quad (18)$$

The feedforward signal is switched off $u_2(t) = 0$ if reference signal $n(t)$ is not available. Minimizing $J(kT) \approx E\{p_e^2 | \boldsymbol{\theta}\}$ can be shown mathematically equivalent to minimizing the H_2 norm from $n(t)$ to $p_e(t)$ by tuning $\boldsymbol{\theta}$.¹⁰ It is possible to apply available system identification algorithms to estimate \mathbf{A} , \mathbf{B}_a , \mathbf{B}_p , \mathbf{C}_e , and \mathbf{C}_f . If online estimates are accurate, the SLANC system may set $\varepsilon = 1$ and apply H_2/H_∞ control algorithms^{10,11,13} to optimize \mathbf{A}_c , \mathbf{B}_c , \mathbf{C}_c , and \mathbf{D}_c . This is a possible version of indirect adaptive control and the dashed tuning block in Fig. 1.

When the reference signal is not available, estimation accuracy is a nontrivial issue.^{7,12} The primary source $n(t)$ causes identification errors if it is not available to the ANC system. Closed-loop stabilities of indirect adaptive controllers are not guaranteed when online estimates of \mathbf{A} , \mathbf{B}_a , \mathbf{B}_p , \mathbf{C}_e , and \mathbf{C}_f are not reliable. The SLANC system is able to deal with such a case. It is represented by the solid tuning block in Fig. 1. Switching between the two tuning blocks depends on online values of $J(kT)$.

IV. SLANC MECHANISM

Although the full value of $J(kT)$ is computed periodically with Eq. (15), partial value of $J(kT)$ is available in every step of summation. If closed-loop stability is threatened, the magnitude of $p_e(t)$ grows rapidly and so does partial or full value of $J(kT)$. Whenever partial or full value of $J(kT)$ exceeds a conservatively preset threshold value, the SLANC system will (a) stabilize the closed loop and (b) optimize \mathbf{A}_c , \mathbf{B}_c , \mathbf{C}_c , and \mathbf{D}_c without using estimates of \mathbf{A} , \mathbf{B}_a , \mathbf{B}_p , \mathbf{C}_e , and \mathbf{C}_f . This study focuses on the worst case when $n(t)$ is unavailable and so severe that results of online identification are not reliable to ensure closed-loop stability.

A. Stabilizing the closed loop

The first task of the SLANC system is to stabilize the closed-loop system. Initially, the dashed tuning block is active with $\varepsilon = 1$, presuming that estimates of \mathbf{A} , \mathbf{B}_a , \mathbf{B}_p , \mathbf{C}_e , and \mathbf{C}_f are accurate. When partial or full value of $J(kT)$

grows out of bound, the system realizes that estimates of \mathbf{A} , \mathbf{B}_a , \mathbf{B}_p , \mathbf{C}_e , and \mathbf{C}_f are not reliable. It switches from the dashed tuning block to the solid counterpart. Tuning ε becomes the only option to ensure closed-loop stability. The effects may be analyzed with help of positive definite function,^{7,10,11}

$$L(t) = \mathbf{v}^T(t)\mathbf{P}\mathbf{v}(t) + \mathbf{w}^T(t)\mathbf{w}(t), \quad (19)$$

where \mathbf{P} is the positive definite matrix in Eq. (12).

$$\begin{aligned} L(t+1) - L(t) &= \begin{bmatrix} \mathbf{v}(t+1) \\ \mathbf{w}(t+1) \end{bmatrix}^T \begin{bmatrix} \mathbf{P} & \\ & \mathbf{I} \end{bmatrix} \begin{bmatrix} \mathbf{v}(t+1) \\ \mathbf{w}(t+1) \end{bmatrix} - \begin{bmatrix} \mathbf{v}(t) \\ \mathbf{w}(t) \end{bmatrix}^T \begin{bmatrix} \mathbf{P} & \\ & \mathbf{I} \end{bmatrix} \begin{bmatrix} \mathbf{v}(t) \\ \mathbf{w}(t) \end{bmatrix} \\ &= \begin{bmatrix} \mathbf{v}(t) \\ \mathbf{w}(t) \end{bmatrix}^T \begin{bmatrix} \mathbf{A}^T\mathbf{P}\mathbf{A} - \mathbf{P} + \varepsilon\mathbf{R}_1 & \varepsilon\mathbf{R}_2 \\ \varepsilon\mathbf{R}_2^T & \varepsilon^2(\mathbf{A}_c^T\mathbf{A}_c + \mathbf{C}_c^T\mathbf{B}_a^T\mathbf{P}\mathbf{B}_a\mathbf{C}_c) - \mathbf{I} \end{bmatrix} \begin{bmatrix} \mathbf{v}(t) \\ \mathbf{w}(t) \end{bmatrix}. \end{aligned} \quad (20)$$

It can be verified that both $\mathbf{R}_1 = \mathbf{A}^T\mathbf{P}\mathbf{B}_a\mathbf{D}_c\mathbf{C}_f + \mathbf{C}_f^T\mathbf{D}_c^T\mathbf{B}_a^T\mathbf{P}\mathbf{A} + \varepsilon(\mathbf{C}_f^T\mathbf{D}_c^T\mathbf{B}_a^T\mathbf{P}\mathbf{B}_a\mathbf{D}_c\mathbf{C}_f + \mathbf{C}_f^T\mathbf{B}_c^T\mathbf{B}_c\mathbf{C}_f)$ and $\mathbf{R}_2 = (\mathbf{A} + \varepsilon\mathbf{B}_a\mathbf{D}_c\mathbf{C}_f)^T \times \mathbf{P}\mathbf{B}_a\mathbf{C}_c + \varepsilon\mathbf{C}_f^T\mathbf{B}_c^T\mathbf{A}_c$ are bounded matrices. As $\varepsilon \rightarrow 0$, one can see that

$$\begin{aligned} L(t+1) - L(t) &\rightarrow \begin{bmatrix} \mathbf{v}(t) \\ \mathbf{w}(t) \end{bmatrix}^T \begin{bmatrix} \mathbf{A}^T\mathbf{P}\mathbf{A} - \mathbf{P} & \\ & -\mathbf{I} \end{bmatrix} \begin{bmatrix} \mathbf{v}(t) \\ \mathbf{w}(t) \end{bmatrix} \\ &= -\mathbf{v}^T(t)\mathbf{Q}\mathbf{v}(t) - \mathbf{w}^T(t)\mathbf{w}(t) < 0, \end{aligned} \quad (21)$$

where Eq. (12) has been substituted.

Equation (21) implies an exponentially decreasing $L(t)$ (magnitudes of closed-loop eigenvalues are smaller than one^{7,10,11}), if ε is sufficiently small and yet different from zero. As a result, a SLANC system can stabilize the closed-loop system by (1) turning off $u_2(t)$ and (2) reducing ε and restarting Eq. (15) whenever partial or full value of $J(kT)$ exceeds a conservatively preset threshold.

B. Controller optimization

If $J(kT)$ is found bounded within the preset threshold, the closed-loop system is detected to be stable. A SLANC system will stop reducing ε and switch to the second task of optimizing \mathbf{A}_c , \mathbf{B}_c , \mathbf{C}_c , and \mathbf{D}_c . In Eq. (16), an one-to-one mapping is created to map elements of \mathbf{A}_c , \mathbf{B}_c , \mathbf{C}_c , and \mathbf{D}_c to elements of $\boldsymbol{\theta}$. If estimates of \mathbf{A} , \mathbf{B}_a , \mathbf{B}_p , \mathbf{C}_e , and \mathbf{C}_f are reliable and dimension of \mathbf{A}_c is larger than or equal to dimension of \mathbf{A} , there exists an optimal $\boldsymbol{\theta}_{\text{opt}}$ that minimizes $J(kT, \boldsymbol{\theta}) \approx E\{p_e^2 | \boldsymbol{\theta}\}$.^{10,13} If estimates of \mathbf{A} , \mathbf{B}_a , \mathbf{B}_p , \mathbf{C}_e , and \mathbf{C}_f are unreliable, however, the only way to optimize $\boldsymbol{\theta}$ is trial-and-error. The SLANC system works periodically at the beginning of the $(2k+1)$ th averaging period of Eq. (15). It is based on two learning rules. The first one is random learning

$$\boldsymbol{\theta}(2k+1) = \boldsymbol{\theta}(2k) + \delta\boldsymbol{\theta}(2k), \quad (22)$$

where $\boldsymbol{\theta}(2k)$ contains parameters of the best available guess; $\boldsymbol{\theta}(2k+1)$ is a tentative parameter vector; and $\delta\boldsymbol{\theta}(2k)$ is a randomly generated vector. At the end of $(2k+1)$ th averaging

If a stability threat is detected, $u_2(t)=0$ is the first action of the SLANC system. Stability of a discrete-time linear system like Eq. (17) may be analyzed using $L(t+1)-L(t)$ by ignoring bounded inputs [$n(t)=0$ in this particular case].^{7,10,11} As a result, Eq. (17) becomes

$$\begin{bmatrix} \mathbf{v}(t+1) \\ \mathbf{w}(t+1) \end{bmatrix} = \begin{bmatrix} \mathbf{A} + \varepsilon\mathbf{B}_a\mathbf{D}_c\mathbf{C}_f & \varepsilon\mathbf{B}_a\mathbf{C}_c \\ \varepsilon\mathbf{B}_c\mathbf{C}_f & \varepsilon\mathbf{A}_c \end{bmatrix} \begin{bmatrix} \mathbf{v}(t) \\ \mathbf{w}(t) \end{bmatrix}.$$

One may use the above-presented equation to obtain

period of Eq. (15), the system either updates $\boldsymbol{\theta}(2k) = \boldsymbol{\theta}(2k+1)$ if $J[2kT, \boldsymbol{\theta}(2k)] > J[(2k+1)T, \boldsymbol{\theta}(2k+1)]$ or otherwise keeps $\boldsymbol{\theta}(2k)$ unchanged. Although in most cases $\boldsymbol{\theta}(2k)$ is the winner of the previous competition, $J[2kT, \boldsymbol{\theta}(2k)]$ is still retested in each new competition since $\boldsymbol{\theta}(2k)$ could represent an unstable controller if parameters of the sound field change suddenly.

Unlike recursive system identifications algorithms, which update the controller in every δt s, the SLANC system waits every $2T\delta t \gg \delta t$ s before it updates $\boldsymbol{\theta}(2k) = \boldsymbol{\theta}(2k+1)$ if $J[2kT, \boldsymbol{\theta}(2k)] > J[(2k+1)T, \boldsymbol{\theta}(2k+1)]$. Otherwise $\boldsymbol{\theta}(2k)$ remains unchanged after $2T\delta t$ s of testing. The value of T is sufficiently large such that $J[2kT, \boldsymbol{\theta}(2k)] \approx E\{p_e^2 | \boldsymbol{\theta}(2k)\}$ and $J[(2k+1)T, \boldsymbol{\theta}(2k+1)] \approx E\{p_e^2 | \boldsymbol{\theta}(2k+1)\}$ when $n(t)$ is stationary and ergodic. If magnitude of the incremental vector $\delta\boldsymbol{\theta}(2k)$ is small enough, the learning process will reach at least a local minimum in the landscape of $E\{p_e^2 | \boldsymbol{\theta}\}$, since each update makes $E\{p_e^2 | \boldsymbol{\theta}\}$ smaller than before or at least unchanged.

It is very difficult to evaluate the probability of $J[\boldsymbol{\theta}(2k)] > J[\boldsymbol{\theta}(2k+1)]$ that depends on many factors including primary noise $n(t)$, locations of sensors and speakers, or even the initial values of $\boldsymbol{\theta}$, etc. It is therefore very difficult to predict the convergence speed of random learning. Let $\theta_i(k)$ be the i th element of vector $\boldsymbol{\theta}(k)$, the SLANC system uses $\delta J(k) = J[(k+1)T, \boldsymbol{\theta}(k+1)] - J[kT, \boldsymbol{\theta}(k)]$ and $\boldsymbol{\theta}(k+1) - \boldsymbol{\theta}(k)$ to estimate the gradient vector

$$\mathbf{g}^T = \begin{bmatrix} \frac{\partial J}{\partial \theta_1} & \frac{\partial J}{\partial \theta_2} & \cdots & \frac{\partial J}{\partial \theta_N} \end{bmatrix},$$

such that $\delta J(k) = \mathbf{g}^T[\boldsymbol{\theta}(k+1) - \boldsymbol{\theta}(k)]$ when magnitudes of $\boldsymbol{\theta}(k+1) - \boldsymbol{\theta}(k)$ are sufficiently small. Approximation error

$$\begin{aligned} e(k) &= \delta J(k) - \mathbf{g}^T(k)[\boldsymbol{\theta}(k+1) - \boldsymbol{\theta}(k)] \\ &= [\mathbf{g} - \mathbf{g}(k)]^T[\boldsymbol{\theta}(k+1) - \boldsymbol{\theta}(k)] \\ &= [\boldsymbol{\theta}(k+1) - \boldsymbol{\theta}(k)]^T[\mathbf{g} - \mathbf{g}(k)] \end{aligned} \quad (23)$$

is used to measure the accuracy of estimated gradient $\mathbf{g}(k)$. Although the true gradient \mathbf{g} is never known, $e(k) = \delta J(k) - \mathbf{g}(k)^T[\boldsymbol{\theta}(k+1) - \boldsymbol{\theta}(k)]$ can be obtained at the end of $(k+1)$ th test period using $\delta J(k) = J[(k+1)T, \boldsymbol{\theta}(k+1)] - J[kT, \boldsymbol{\theta}(k)]$. A positive definite function

$$V(k) = [\mathbf{g} - \mathbf{g}(k)]^T [\mathbf{g} - \mathbf{g}(k)] \quad (24)$$

is used to represent estimation error of the gradient. Similar to identity $a^2 - b^2 = (a-b)(a+b)$, it can be derived that

$$V(k+1) - V(k) = [\mathbf{g}(k) - \mathbf{g}(k+1)]^T [2\mathbf{g} - \mathbf{g}(k+1) - \mathbf{g}(k)]. \quad (25)$$

A recursive algorithm

$$\mathbf{g}(k+1) = \mathbf{g}(k) + \frac{e(k)[\boldsymbol{\theta}(k+1) - \boldsymbol{\theta}(k)]}{\|\boldsymbol{\theta}(k+1) - \boldsymbol{\theta}(k)\|^2} \quad (26)$$

is proposed in this study to estimate $\mathbf{g}(k)$. It is mathematically equivalent to

$$\mathbf{g}(k+1) - \mathbf{g}(k) = \frac{e(k)[\boldsymbol{\theta}(k+1) - \boldsymbol{\theta}(k)]}{\|\boldsymbol{\theta}(k+1) - \boldsymbol{\theta}(k)\|^2}, \quad (27)$$

and

$$2\mathbf{g} - \mathbf{g}(k+1) - \mathbf{g}(k) = 2[\mathbf{g} - \mathbf{g}(k)] - \frac{e(k)[\boldsymbol{\theta}(k+1) - \boldsymbol{\theta}(k)]}{\|\boldsymbol{\theta}(k+1) - \boldsymbol{\theta}(k)\|^2}. \quad (28)$$

If one substitutes Eqs. (27) and (28) into Eq. (25), the result will be

$$V(k+1) - V(k) = - \frac{e(k)[\boldsymbol{\theta}(k+1) - \boldsymbol{\theta}(k)]^T}{\|\boldsymbol{\theta}(k+1) - \boldsymbol{\theta}(k)\|^2} \left\{ 2[\mathbf{g} - \mathbf{g}(k)] - \frac{e(k)[\boldsymbol{\theta}(k+1) - \boldsymbol{\theta}(k)]}{\|\boldsymbol{\theta}(k+1) - \boldsymbol{\theta}(k)\|^2} \right\}. \quad (29)$$

Substituting Eq. (23) into Eq. (29), one can finish the derivation with

$$V(k+1) - V(k) = \frac{-e^2(k)}{\|\boldsymbol{\theta}(k+1) - \boldsymbol{\theta}(k)\|^2} \leq 0. \quad (30)$$

It indicates monotonous decrease of $V(k) = [\mathbf{g} - \mathbf{g}(k)]^T [\mathbf{g} - \mathbf{g}(k)]$ until $e(k) \rightarrow 0$.

Upon the convergence of $\mathbf{g}(k) \approx \mathbf{g}$, which is signaled by $e(k) \rightarrow 0$, the learning rule may be changed from Eq. (22) to

$$\begin{aligned} \boldsymbol{\theta}(2k+1) &= \boldsymbol{\theta}(2k) - \mu\mathbf{g}(2k) + \delta\boldsymbol{\theta}(2k) \quad \text{or} \quad \boldsymbol{\theta}(2k+1) \\ &- \boldsymbol{\theta}(2k) = -\mu\mathbf{g}(2k) + \delta\boldsymbol{\theta}(2k), \end{aligned} \quad (31)$$

where μ is a small positive constant. One may use Eq. (31) and the gradient to predict

$$\begin{aligned} \delta J(2k) &= \mathbf{g}^T [\boldsymbol{\theta}(2k+1) - \boldsymbol{\theta}(2k)] = -\mu\mathbf{g}^T \mathbf{g}(2k) \\ &+ \mathbf{g}^T \delta\boldsymbol{\theta}(2k). \end{aligned} \quad (32)$$

Due to the convergence of $\mathbf{g}(2k) \approx \mathbf{g}$, it is expected that $\mathbf{g}^T \mathbf{g}(2k) > 0$ and hence

$$E\{\delta J(2k)\} = E\{\mathbf{g}^T [\boldsymbol{\theta}(2k+1) - \boldsymbol{\theta}(2k)]\} = -\mu\mathbf{g}^T \mathbf{g}(2k) < 0, \quad (33)$$

where all elements of $\delta\boldsymbol{\theta}(k)$ are zero-mean random numbers such that $E\{\mathbf{g}^T \delta\boldsymbol{\theta}(2k)\} = 0$. The statistical expectation of the second learning rule is to reduce $J(kT)$ in the averaging period of Eq. (15), as indicated by Eq. (33).

By incorporating online estimation of gradient vector, the second learning rule converges faster since it increases probability of $J[\boldsymbol{\theta}(2k)] > J[\boldsymbol{\theta}(2k+1)]$ as hinted by Eq. (33). However, it is still very difficult to evaluate the probability of $J[\boldsymbol{\theta}(2k)] > J[\boldsymbol{\theta}(2k+1)]$ and the convergence speed of improved self-learning. If online system identification is an optional part of a SLANC system, the identification algorithm never stops even if indirect adaptive control is not stable. The SLANC system keeps using estimates \mathbf{A} , \mathbf{B}_a , \mathbf{B}_p , \mathbf{C}_f , and \mathbf{C}_e to update the indirect adaptive controller in a hope that these matrices will eventually become reliable. Accuracy and speed of convergence of \mathbf{A} , \mathbf{B}_a , \mathbf{B}_p , \mathbf{C}_f , and \mathbf{C}_e depend on specific online system identification algorithms. Although there are many available system identification algorithms, it is difficult to say which one is best in terms of accuracy and speed of convergence even for linear systems without disturbances. In many ANC applications, $n(t)$ is a strong disturbance and it is more difficult to predict how long it takes for online estimates of \mathbf{A} , \mathbf{B}_a , \mathbf{B}_p , \mathbf{C}_f , and \mathbf{C}_e to become reliable. Periodically, the system allocates test periods of Eq. (15) for the indirect adaptive controller to challenge the best available controller. Performances of controllers are judged by the objective function at the end of test periods. The system keeps the winner that has a smaller $J(*)$ in the competition.

Since an indirect adaptive controller may be unstable if estimates \mathbf{A} , \mathbf{B}_a , \mathbf{B}_p , \mathbf{C}_f , and \mathbf{C}_e are unreliable, the SLANC system will reduce ε and stabilize the indirect adaptive controller if it produces a growing $J(*)$. Once online estimates become accurate, the indirect controller will be optimized by available H_2/H_∞ control algorithms.^{10,11,13} It is expected to be adopted by the SLANC system after winning a competition with a smaller $J(*)$.

C. Combination with feedforward control

When $J(kT)$ is found no longer decreasing after repeated testing of controllers, the SLANC system may stop updating the feedback controller by fixing on a controller that produces a smaller $J(kT)$ in the most recent test period. The SLANC system then switches to a third task of incorporating feedforward control if reference signal $n(t)$ is available. The closed-loop system, represented by Eqs. (17) and (18), may be expressed in the discrete-time z -transform domain as

$$p_e(z) = P(z)n(z) + S(z)u_2(z), \quad (34)$$

where $p_e(z)$, $n(z)$, and $u_2(z)$ are z -transform versions of $p_e(t)$, $n(t)$, and $u_2(t)$, respectively; primary path $P(z)$ and secondary path $S(z)$ transfer functions can be obtained from state space models^{7,10} as

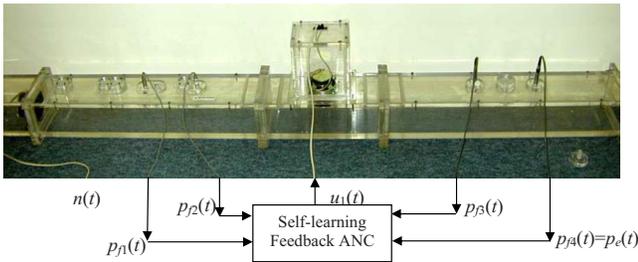


FIG. 2. (Color online) Experiment setup in a 2 m duct.

$$P(z) = [C_e] \begin{bmatrix} zI - A - \varepsilon B_a D_c C_f & -\varepsilon B_a C_c \\ -\varepsilon B_c C_f & zI - \varepsilon A_c \end{bmatrix}^{-1} [B_p], \quad (35)$$

and

$$S(z) = [C_e] \begin{bmatrix} zI - A - \varepsilon B_a D_c C_f & -\varepsilon B_a C_c \\ -\varepsilon B_c C_f & zI - \varepsilon A_c \end{bmatrix}^{-1} [B_a]. \quad (36)$$

Both $P(z)$ and $S(z)$ contain parameters of the feedback controller. Since the feedback controller is tested and updated in online operation, it is not possible to obtain $P(z)$ and $S(z)$ by initial offline identification. A recently developed algorithm, known as orthogonal adaptation,^{14,15} can be combined with a SLANC system to generate destructive interference. Let $C_2(z)$ denote transfer function of a feedforward controller such that $u_2(z) = C_2(z)n(z)$, then orthogonal adaptation is able to minimize H_2 norm $\|P(z) + S(z)C_2(z)\|_2$ using online estimates of $P(z)$ and $S(z)$. Details of orthogonal adaptation have been published elsewhere^{14,15} and omitted here.

V. EXPERIMENT

An experiment was conducted to test a SLANC system in the worst case when self-learning is the only option for stable and optimal operation. Figure 2 illustrates the experimental setup in a 2 m duct with a cross-sectional area of $12 \times 15 \text{ cm}^2$. The primary source was a 4 in. speaker placed at the upstream end of the duct. It was excited by the pseudorandom noise. The secondary actuator was a 4 in. speaker placed at the middle of the duct. Four feedback sensors were placed on both sides of the actuator. The most downstream sensor was also the error sensor.

The system sampling rate was 2500 Hz. Dimensions of A_c , B_c , C_c , and D_c were 200×200 , 200×4 , 1×200 , and 1×4 , respectively. Parameters of A , B_a , B_p , C_e , and C_f were completely unknown to the SLANC system. Eigenvalues of A are all inside the unit circle centered at the origin of the complex plane, since the sound field is open-loop stable. The objective function was computed using Eq. (15) with $T = 200\,000$ samples. Analog signals in the system were low-pass filtered with a cutoff frequency of 800 Hz before digitized into the SLANC system. The SLANC system was programmed in standard C language and implemented on a dSPACE 1103 board. Although it is possible to combine the SLANC system with indirect adaptive control, the option

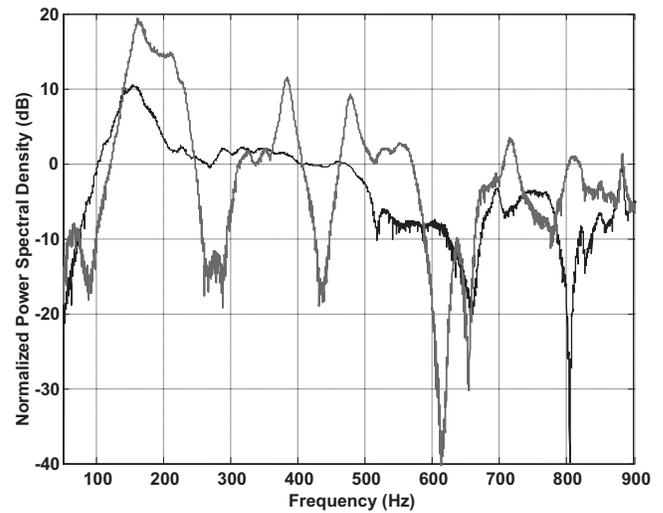


FIG. 3. Normalized power spectral densities of error signal when SLANC was off (gray) and on (black).

was disabled to focus on the worst case exclusively. Reference signal $n(t)$ was not available to the controller. Only the feedback control part was tested in the experiment.

Two sets of experimental data were collected for the cases with/without control, respectively. Each set of data was the power spectral density (PSD) of the error signal normalized by the PSD of the primary noise signal. The two normalized PSDs are plotted in Fig. 3, where the black and gray curves represent, respectively, normalized PSD of the error signal for the cases with/without active control. When the controller was off, resonant effects are evidently seen in the gray PSD with significant resonant peaks and antiresonant dips. Since the reference signal was not available to the SLANC system in the experiment, feedback control was only able to introduce active damping to reduce resonant effects. It reduced resonant peaks and filled up antiresonant dips simultaneously, as demonstrated by the black PSD in Fig. 3. The SLANC system worked very well to optimize active damping in a wide frequency range (20–800 Hz), even when parameters of A , B_a , B_f , C_f , and C_e were completely unavailable.

Self-learning control is the major difference between a SLANC system and other available MIANC systems. The experiment was intended to test the feedback part of a SLANC system in a worst case when the reference signal was unavailable and online system identification results were unreliable. The feedforward part and indirect adaptive control were not tested because both options are not results of this study. Compared with available feedback MIANC systems such as direct rate feedback control or active resonators, the SLANC system tolerates dynamic uncertainties in the ANC system, avoids sensing near fields, and is able to minimize objective function $J(kT)$, as verified by the experiment.

VI. CONCLUSIONS

The major difference between a SLANC system and available MIANC systems is self-learning in the worst case when (i) model parameters of the sound field are unreliable due to online estimation errors and (ii) reference signal is

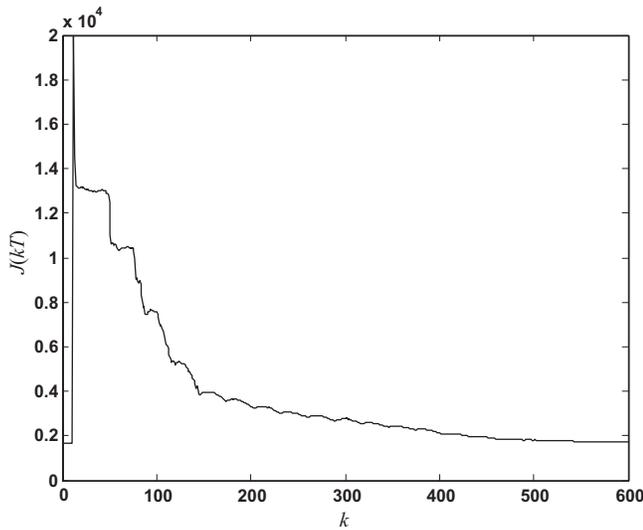


FIG. 4. Values of $J(kT)$ as a function of k .

unavailable. The SLANC system tolerates dynamic uncertainties in sound fields to stabilize the closed-loop system by tuning controller parameters.

A curve of $J(kT)$ is plotted in Fig. 4 as a function of k in the worst case without online system identification. The controller started with parameters learned previously. Its parameters were replaced with random numbers when $k=10$. The system took a very large number of k to converge. This is a drawback of self-learning and also a reason why indirect adaptive control is incorporated in Fig. 1. Available system identification algorithms converge quickly and accurately in the absence of disturbances like $n(t)$. When $n(t)$ acts as the disturbance, there is no guarantee on the accuracy of parameter estimates. If estimates of \mathbf{A} , \mathbf{B}_a , \mathbf{B}_p , \mathbf{C}_e , and \mathbf{C}_f are accurate, indirect adaptive control is optimal; otherwise it may be unstable. Self-learning control is a stable backup whenever indirect adaptive control is unstable. Since the system allocates test periods to both tuning blocks periodically, indirect adaptive control is expected to win a competition whenever it is nearly optimal. Afterwards, elements of $\boldsymbol{\theta}(2k)$ become parameters of the indirect adaptive controller. Elements of $\boldsymbol{\theta}(2k+1)$ are either (i) slightly modified elements of $\boldsymbol{\theta}(2k)$ by Eq. (31) or (ii) parameters of a fresher version of the indirect adaptive controller. In case (ii), $\boldsymbol{\theta}(2k+1)$ is not necessarily better than $\boldsymbol{\theta}(2k)$ due to estimation errors. If $\boldsymbol{\theta}(2k+1)$ represents an unstable controller, the SLANC system will stabilize the closed loop by reducing ε . If Eq. (16) were exact, the competitions would either improve $\boldsymbol{\theta}(2k)$ if $E\{p_e^2|\boldsymbol{\theta}(2k)\} > E\{p_e^2|\boldsymbol{\theta}(2k+1)\}$ or otherwise keep $\boldsymbol{\theta}(2k)$ unchanged. Due to finite T and approximation errors in Eq.

(16), values of $J(kT, \boldsymbol{\theta})$ fluctuate slightly for different k even when a constant $\boldsymbol{\theta}$ represents a stable controller. The fluctuation may cause sporadic false updates of $\boldsymbol{\theta}(2k)$, but the SLANC system generally remains optimal or nearly optimal until parameters of the sound field change and the entire process starts over again.

If the reference signal is available, a SLANC system may be combined with a feedforward controller to apply both destructive interference and active damping to sound fields. Experimental results are presented to demonstrate the performance of a SLANC system in the worst case. The SLANC system proves to be a simple and stable tool for many feedback ANC systems to deal with the worst case discussed in this study.

ACKNOWLEDGMENTS

The writer thanks the reviewers for their penetrating comments and suggestions that led to an improved version of the manuscript. This project was partially supported by Internal Grant No. G-U392 from the Hong Kong Polytechnic University.

- ¹C. H. Hansen and S. D. Snyder, *Active Control of Noise and Vibration* (E and FN Spon, London, 1997).
- ²P. A. Nelson and S. J. Elliott, *Active Control of Sound* (Academic, London, 1992).
- ³R. L. Clark and D. G. Cole, "Active damping of enclosed sound fields through direct rate feedback control," *J. Acoust. Soc. Am.* **97**, 1710–1716 (1995).
- ⁴H. R. Pota and A. G. Kelkar, "Modeling and control of acoustic ducts," *ASME J. Vib. Acoust.* **123**, 2–10 (2001).
- ⁵J. D. Kemp and R. L. Clark, "Noise reduction in a launch vehicle fairing using actively tuned loudspeakers," *J. Acoust. Soc. Am.* **113**, 1986–1994 (2003).
- ⁶J. B. Bisnette, J. S. Viperman, and D. D. Budny, "Active noise control using damped resonator filters," *J. Acoust. Soc. Am.* **113**, 2228–2234 (2003).
- ⁷J. Dorsey, *Continuous and Discrete Control Systems: Modeling, Identification, Design, and Implementation* (McGraw-Hill, Boston, 2002).
- ⁸D. E. Hall, *Basic Acoustics* (Wiley, New York, 1987).
- ⁹S. Liu, J. Yuan, and K. Y. Fung, "Robust active control of broadband noise in finite ducts," *J. Acoust. Soc. Am.* **111**, 2727–2734 (2002).
- ¹⁰S. Boyd, L. El Ghaoui, E. Feron, and V. Balakrishnan, *Linear Matrix Inequalities in Systems and Control Theory* (SIAM Books, Philadelphia, 1994).
- ¹¹B. A. Frances, "A course in H_∞ control theory," in *Lecture Notes in Control and Information Sciences*, edited by M. Thoma and A. Wyner (Springer, New York, 1987).
- ¹²G. C. Goodwin and K. S. Sin, *Adaptive Filtering, Prediction and Control* (Prentice-Hall, Englewood Cliffs, NJ, 1984).
- ¹³P. P. Khargonekar and M. A. Rotea, "Mixed H_2/H_∞ control: A convex optimization approach," *IEEE Trans. Autom. Control* **39**, 824–837 (1991).
- ¹⁴J. Yuan, "Orthogonal adaptation for active noise control," *J. Acoust. Soc. Am.* **120**, 204–210 (2006).
- ¹⁵J. Yuan, "Orthogonal adaptation for multichannel feedforward control," *J. Acoust. Soc. Am.* **120**, 3723–3729 (2006).